

Supporting information

Epitaxial growth of bismuth oxyhalide thin films using mist CVD at atmospheric pressure

Zaichun Sun,^a Daichi Oka,^{ a} and Tomoteru Fukumura^{a,b}*

^a Department of Chemistry, Graduate School of Science, Tohoku University, 6-3 Aramaki Aza Aoba, Aoba, Sendai, 980-8578, Japan

^b Advanced Institute for Materials Research and Core Research Cluster, Tohoku University, 2-1-1 Katahira, Aoba, Sendai, 980-8577, Japan

Materials and Methods

N,N-dimethylformamide (DMF, purity: 99.5%; Wako) solutions of BiCl₃ (purity: 99.99%; Kojundo Chemical Lab., 0.005 mol/L), BiBr₃ (purity: 99.95%; Kojundo Chemical Lab., 0.02 mol/L), and BiI₃ (purity: 99.99%; Kojundo Chemical Lab., 0.04 mol/L) were used as the precursor solutions. Each solution was nebulized into microscale mist and then transferred by N₂ gas with the flow rates of 3.0, 0.8, and 0.4 L/min, for BiOCl, BiOBr, and BiOI, respectively. For diluting the mist during the deposition, N₂ gas with the flow rate of 0.5 L/min for BiOCl and O₂ gas with that of 0.1 L/min for BiOBr and BiOI were supplied. The substrates were placed in a quartz tube heated at 250 – 400 °C by a tubular furnace. The crystal structures of the thin films were analyzed by an X-ray diffractometer using Cu K α radiation (D8 Discover, Bruker). The surface morphology was observed by an atomic force microscope (AFM; SPI-4000, Hitachi High Technologies) and a field-emission scanning electron microscope (SEM; JSM-7800F, JEOL). The chemical composition was evaluated with energy dispersive X-ray spectroscopy (EDS) by using an energy dispersive analyzer equipped with the SEM. The chemical states of the constituent elements were investigated with X-ray photoelectron spectroscopy (XPS; AXIS-Ultra DLD, Kratos), where the peak positions were corrected with the C 1s peak at 284.2 eV.

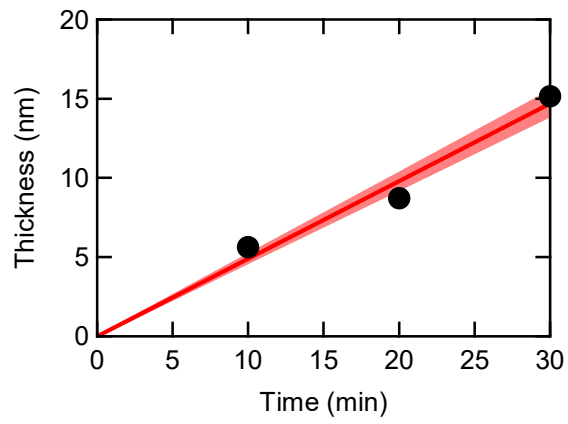


Figure S1. Thickness for BiOI epitaxial thin films as a function of deposition time. The red line denotes a linear fitting with the standard deviation (shaded area).

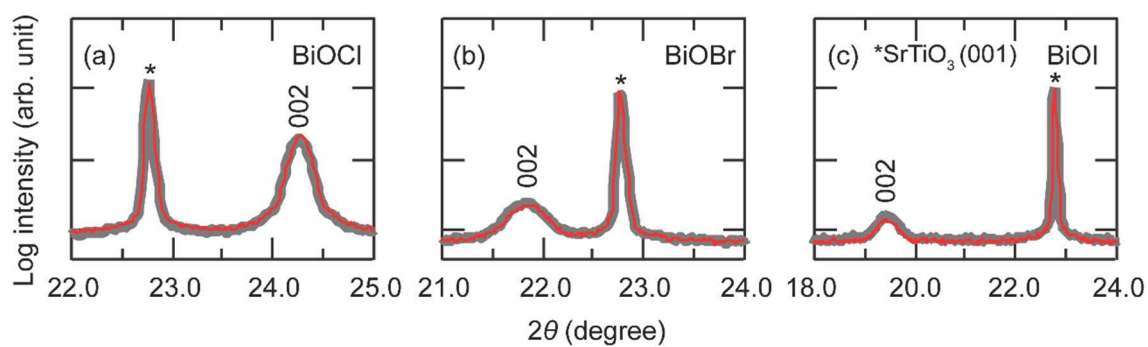


Figure S2. X-ray diffraction $\theta-2\theta$ patterns for (a) BiOCl, (b) BiOBr, and (c) BiOI epitaxial thin films after deposition (thick grey curve) and after 12, 9, and 10 months, respectively, in air (red curve).

Table S1. FWHM of rocking curves around the 003 peaks of BiOCl and BiOBr and the 004 peak of BiOI thin films grown at various temperatures.

	BiOCl	BiOBr	BiOI
250°C	–	0.077°	0.085°
300°C	0.151°	0.087°	0.087°
350°C	0.111°	0.917°	0.153°
400°C	0.106°	–	–

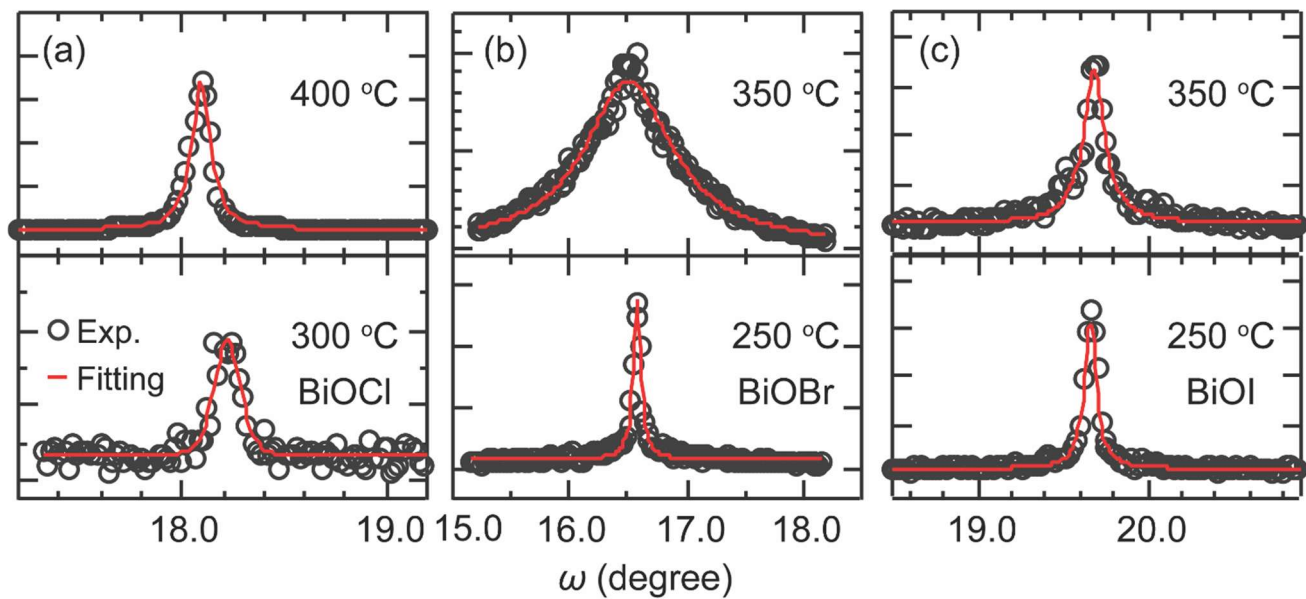


Figure S3. Rocking curves around (a) BiOCl 003, (b) BiOBr 003, and (c) BiOI 004 peaks for BiOX epitaxial thin films grown on STO (001) substrates at various temperatures.

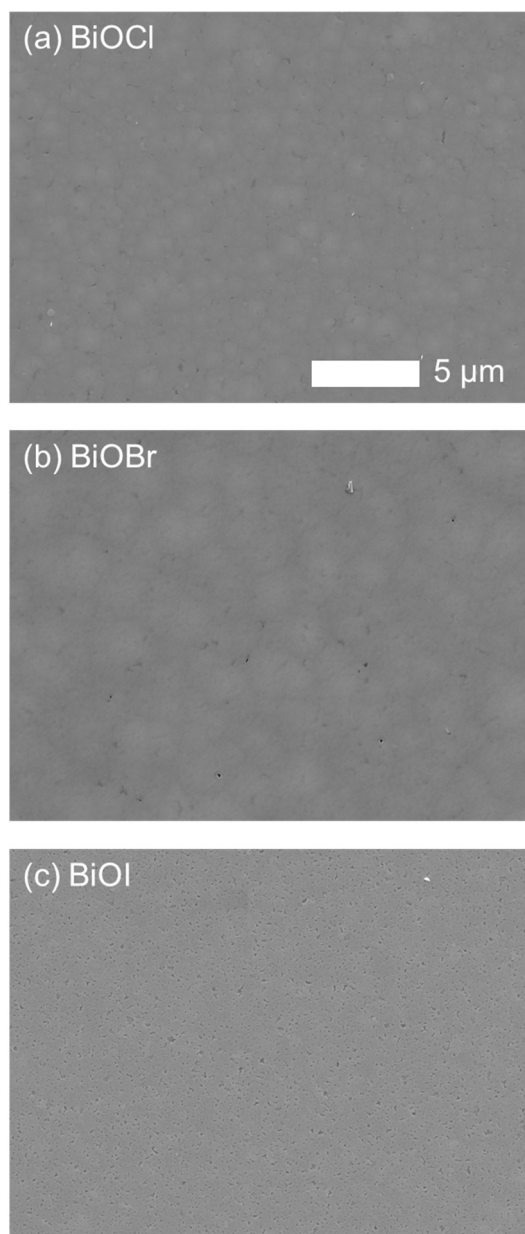


Figure S4. Scanning electron microscope images of (a) BiOCl (b) BiOBr, and (c) BiOI epitaxial thin films grown at the optimum temperatures.

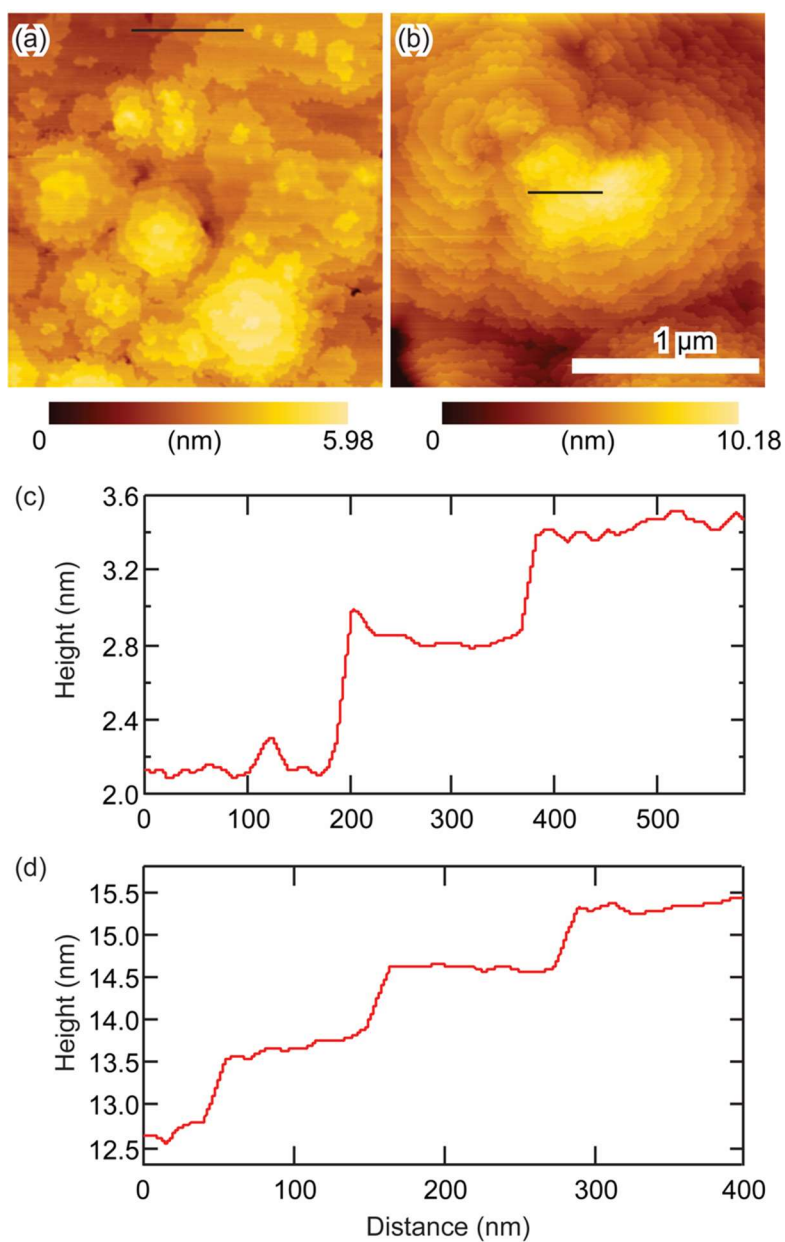


Figure S5. (a, b) Plane-view AFM images of (a) BiOCl and (b) BiOBr epitaxial thin films shown in Fig. 2b and 2e, respectively. (c, d) Line profiles along the black lines in (a) and (b), respectively.

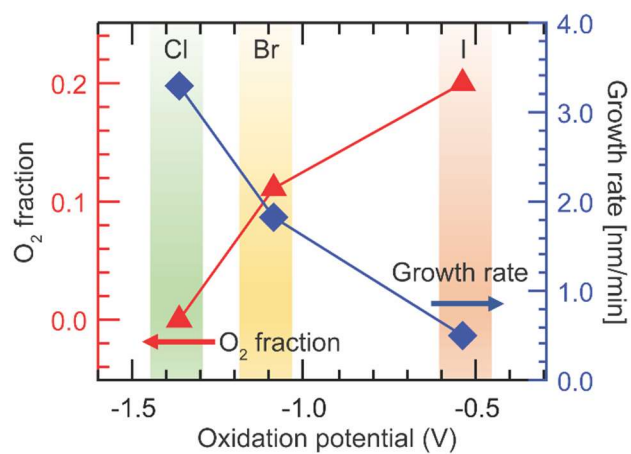


Figure S6. Growth rate and optimum O₂ fraction in the process gas growth rate for BiOX epitaxial thin films plotted against the oxidation potential for the half-reaction: $2X^- \rightarrow X_2 + 2e^-$.

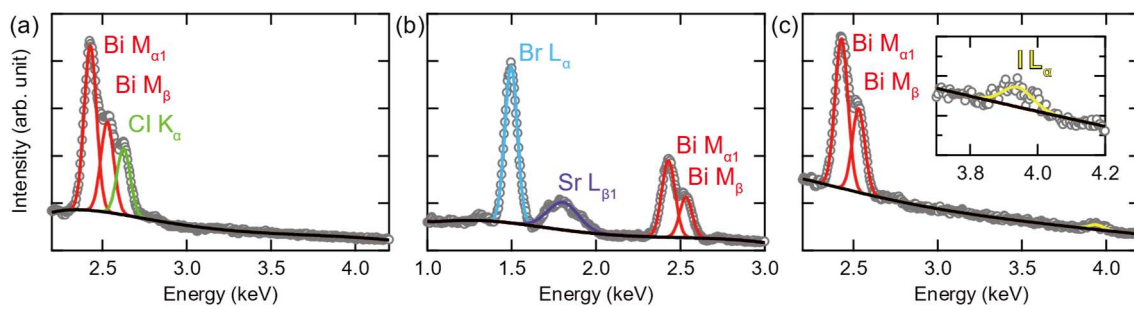


Figure S7. Energy dispersive X-ray spectra for (a) BiOCl, (b) BiOBr, and (c) BiOI epitaxial thin films. Curves show the results of fitting. Inset of (c) shows a magnified view around the $\text{I } L_{\alpha}$ peak.

Table S2. Bi/X composition ratio in BiOX epitaxial thin films quantified from the energy dispersive X-ray spectra in Figure S7.

X	Cl	Br	I
Bi/X ratio	1.08	1.01	0.96

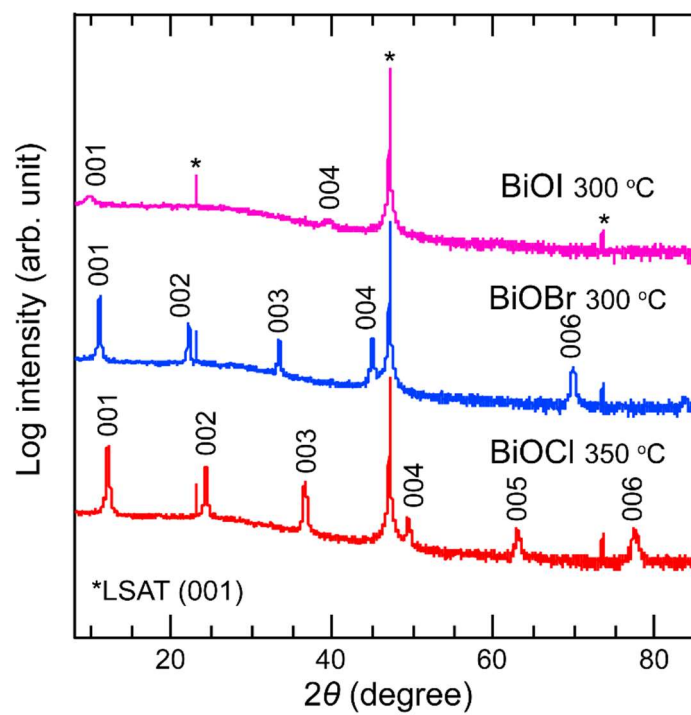


Figure S8. XRD θ - 2θ patterns for BiOCl, BiOBr, and BiOI epitaxial thin films synthesized on LSAT (001) substrates grown at the optimum temperatures.

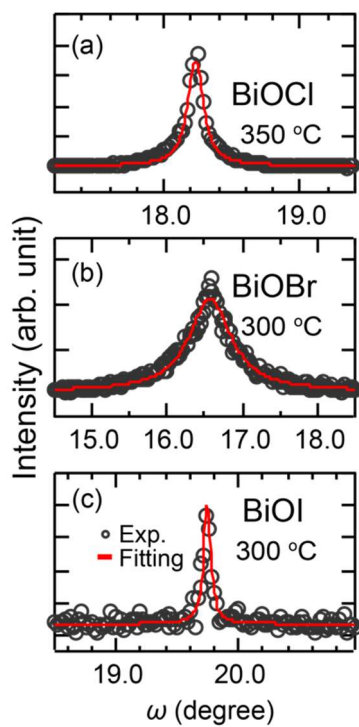


Figure S9. Rocking curves around (d) BiOCl 003, (e) BiOBr 003, and (f) BiOI 004 peaks for BiOX epitaxial thin films grown on LSAT (001) substrates grown at the optimum temperatures.

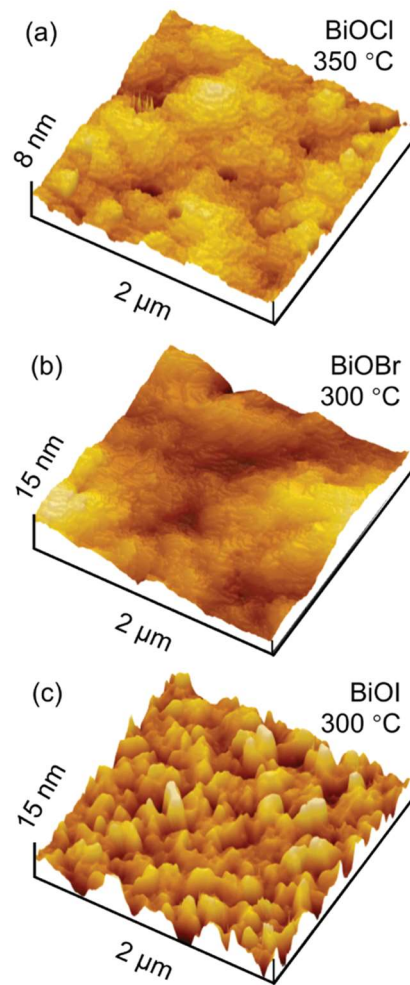


Figure S10. Three-dimensional AFM images of (a) BiOCl, (b) BiOBr, and (c) BiOI epitaxial thin films on LSAT (001) substrates grown at the optimum temperatures.